A macroscopic model of proton transport through the membrane-ionomer interface of a polymer electrolyte membrane fuel cell

Milan Kumar, Brian J. Edwards,[a] and Stephen J. Paddison[a]
Department of Chemical and Biomolecular Engineering University of Tennessee, Knoxville, Tennessee 37996, USA

(Received 3 October 2012; accepted 17 January 2013; published online 13 February 2013)

The membrane-ionomer interface is the critical interlink of the electrodes and catalyst to the polymer electrolyte membrane (PEM); together forming the membrane electrode assembly in current state-of-the-art PEM fuel cells. In this paper, proton conduction through the interface is investigated to understand its effect on the performance of a PEM fuel cell. The water containing domains at this interface were modeled as cylindrical pores/channels with the anionic groups (i.e., $-SO_3^-$) assumed to be fixed on the pore wall. The interactions of each species with all other species and an applied external field were examined. Molecular-based interaction potential energies were computed in a small test element of the pore and were scaled up in terms of macroscopic variables. Evolution equations of the density and momentum of the species (water molecules and hydronium ions) were derived within a framework of nonequilibrium thermodynamics. The resulting evolution equations for the species were solved analytically using an order-of-magnitude analysis to obtain an expression for the proton conductivity. Results show that the conductivity increases with increasing water content and pore radius, and strongly depends on the separation distance between the sulfonate groups and their distribution on the pore wall. It was also determined that the conductivity of two similar pores of different radii in series is limited by the pore with the smaller radius. © *2013 American Institute of Physics*. [http://dx.doi.org/10.1063/1.4789960]

I. INTRODUCTION

Polymer electrolyte membrane (PEM) fuel cells are an efficient alternative source of clean energy for long-term consumption. An essential component controlling the performance of a PEM fuel cell is the membrane electrode assembly (MEA), which is a combination of electrodes, catalysts, ionomer, and membrane. Hydrogen gas is commonly used as the fuel and is oxidized at the platinum catalyst on the anode, thus generating protons and electrons. The electrons move through an external circuit and hydrated protons move through the ionomer and membrane. The transport of protons is strongly dependent on the hydrated morphology of the PEM, and so the exact nature of this morphology is an essential characteristic to be considered in the design of high performance ionomers for commercialization. Having passed through the membrane, the protons react with the electrons and oxygen gas, introduced on the cathode side, producing water, which is the only byproduct of the device.

The MEA may be constructed in various ways. In the glue method,[1] an ionomer ink, which is a solution of ionomer and Pt/carbon catalyst, is used to facilitate good interfacial contact between the electrodes and electrolyte. The membrane is sandwiched between the electrodes and pressed, bringing about changes in the morphology and proton conductivity of the membrane at the interfaces on both sides of the membrane. Both the membrane and interface properties dictate the overall conductivity of protons through the MEA. For example, it has been observed that a thicker membrane can cause an interfacial delamination under freeze/thaw cycles.[2] Furthermore, due to delamination, interfacial resistance increases and proton conductivity decreases.[3] Hence, the study of proton transport through the interfacial regions, not simply through the membrane alone, is critical to obtaining insight into the overall proton conductivity of a PEM fuel cell; however, no models for transport through the interfacial region of the MEA have been presented in the literature.

The interface formed in a MEA, made with a Nafion solution on a Nafion membrane, typically behaves in a similar manner as the membrane; however, the pores in the interfacial region are more permanent, being less affected by factors such as temperature or membrane water content. A number of studies have investigated the transport of species through perfluorosulfonic acid membranes, but modeling of the transport through the interface has largely been overlooked. Presently available macroscopic transport models[4] can primarily be divided into three categories: hydraulic;[5] diffusion;[6] and binary friction,[7] including modifications[8,9] of the dusty gas models.[10] Microscopic or molecular-level models include classical molecular dynamics simulations[11] and a kinetic model based on statistical mechanics.[12,13] The model developed in the present work is based on this nonequilibrium statistical mechanical model. Some continuum models have also been developed that are used to describe transport within the microscopic pores of the membrane.[14,15]

[a]Authors to whom correspondence should be addressed. Electronic addresses: bedward1@utk.edu and spaddison@utk.edu.

In the model developed herein, we have assumed that the Nafion membrane-ionomer interface is a collection of cylindrical pores. The structure of the pore is taken as assumed by Paddison *et al.*[12] The negative charges (sulfonate ions) are uniformly distributed on the wall of the pore. The pore is filled with water, and there is no water-density variation. The flux of water within the pore is zero. The velocity and density of hydronium ions are fixed at the entrance of the pore. The interaction potential energies between hydronium ion–hydronium ion, water–water, hydronium ion–water, sulfonate–hydronium ion, and sulfonate–water are estimated by appropriate methods mentioned in the literature. These interaction potential energies were scaled up to the macroscopic interaction potential energies for a small test element of the pore, and the macroscale Hamiltonian in the element was determined. Continuum transport equations for density and velocity of the species were derived using the Hamiltonian via nonequilibrium thermodynamics modeling.[16] These equations were converted into non-dimensional form and solved analytically for density and velocity variations of the hydronium ions within the pore using an order-of-magnitude analysis. An expression for proton conductivity was derived using the current density in the pore under an applied external electric field.

Realistically, the pores within the membrane and interfacial regions are not cylindrical tubes by any means. However, reasonable estimates of the dimensions of the water containing regions in hydrated PEMs have been obtained with small angle x-ray scattering (SAXS) and from these measurements one may estimate average pore diameter as a function of hydration.[17] Furthermore, the sulfonate groups attached to the membrane material are not likely to be uniformly arranged along the channels formed within the membrane and interface; however a number of them will be correlated with the membrane equivalent weight (EW). Nevertheless, for a given membrane of specified EW, a cylindrical tube with uniformly distributed charges should constitute an excellent model for examining the effects of sulfonate distribution, water content, tube size, etc. on proton transport through a typical membrane pore, and to accurately approximate macroscopic transport properties, such as the overall MEA conductivity.

This paper is divided into three major sections. Section II consists of the derivation of all macroscopic interaction potential energies in a pore element under appropriate assumptions, along with the derivation of the evolution equations for density and velocity of the species in the pore. This section also includes the analytic solution of these evolution equations, subject to appropriate boundary conditions. The values of various pore and material parameters, including pore radius, water content, number of sulfonate groups, and proton diffusion coefficient of the pore, have also been incorporated. This section includes a brief comparison of the model with other models from the literature. The variation of the proton conductivity with respect to pore radius, separation distance between sulfonate groups, and distribution of sulfonate groups along the pore wall is presented in Sec. III. This section also provides an expression for interfacial conductivity. The primary conclusions are discussed in Sec. IV.

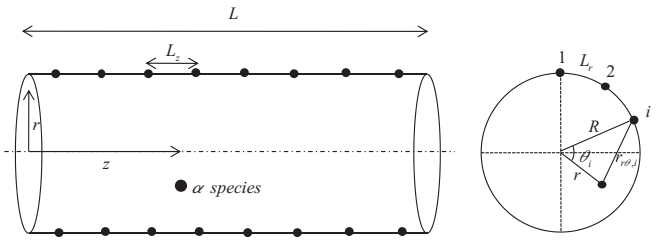

FIG. 1. Interaction of a species, α, with charges on the ith line of a cylinder of length L and radius R. L_z and L_r are the separation distances between two consecutive rings of charges on the axial length and between two consecutive charges in the ring, respectively. The species α is at a radial distance r and is at angle θ_i from the ith line charge. $r_{r\theta,i}$ is the distance of the species from the line charge and is equal to $(R^2 + r^2 - 2Rr\cos(\theta_i))^{1/2}$, where $r = [0, R]$, $\theta_i = [0, 2\pi]$.

II. MATHEMATICAL MODELING

A. Macroscopic potential energies

The densities of the hydronium ions and water molecules are assumed to vary only in the z direction within the pore; hence, the interaction potential energies are functions of the z direction only. Note, however, that we will express most equations in general form in terms of an arbitrary coordinate system $\mathbf{x}$, and then reduce the final equations accordingly later on. Hydronium ions and water molecules move through the pore of a membrane/interface experiencing an electric field due to negatively charged sulfonate anions ($-SO_3^-$) located at the termini of the side-chains. A pore was modeled as a cylindrical tube, as displayed in Fig. 1. The pore has radius R and length L. Approximate values of these quantities can be estimated from SAXS experiments.[17] The lines of charges on the wall are assumed to form $N_L = N'_L + 1$ rings of sulfonate groups, and each ring has N_c sulfonate groups. The separation distance between two consecutive rings is L_z $(=L/N'_L)$. Thus, N'_L is defined as the number of segments along the axial length. The equivalent weight of a particular membrane material provides an estimate of the number of charges within a cylinder of specific dimensions. Although these groups are not likely to be arranged symmetrically within the tubes, nor the pores even cylindrical, the above approximations should allow realistic calculations of membrane-ionomer interfacial transport properties to be obtained.

To calculate the above mentioned interaction potential energies at the continuum level, we focus on a small element of the tube of length L_z at a distance of z from the left end of the tube (Fig. 1). We begin by assuming that the water content of the interface is λ, which is defined as the number of water molecules per sulfonic acid group. If the interface is sufficiently hydrated, all sulfonic acid groups will dissociate their protons to the water molecules forming hydronium ions. Thus, the number of hydronium ions within the pore element is equal to the number of sulfonate groups, N_c, and is related to the macroscopic number density of the hydronium ions at any point $\mathbf{x}$ within the pore element, $\rho_\alpha(\mathbf{x})$, as $\int\int\int \rho_\alpha(\mathbf{x})d\mathbf{x} = N_c$. The mass density is thus defined as $\rho_{m,\alpha} = \rho_\alpha M_\alpha / N_A$, where M_α is the molar mass and N_A is Avogadro's number.

The number of water molecules is $N_c \times (\lambda - 1)$ within the pore element (the remainder of the $N_c \times \lambda$ water

molecules is associated with hydronium ions). The total number of water molecules in the pore is related to the macroscopic number density of water molecules at any point $\mathbf{x}$ in the pore element, $\rho_s(\mathbf{x})$, as $\int\int\int \rho_s(\mathbf{x})d\mathbf{x} = N_c \times (\lambda - 1)$. The mass density of water, $\rho_{m,s}$, is defined analogously to that of the hydronium ions.

A dissociated proton is assumed to exist as a hydronium ion and is free to interact with hydronium ions or water molecules within the pore, as well as with the sulfonate groups distributed along the pore wall. The point charge, q_2, on the wall of the pore may be expressed in terms of the surface charge density, Ω_s, according to $\frac{2\pi RL\Omega_s}{N_L N_c}$. The charge of a hydronium ion is $\frac{F}{N_A}$. The macroscopic potential energies used in the interfacial transport model are developed in terms of previously utilized microscopic potential energy expressions[12] and are summarized in Appendix A.

1. Sulfonate–hydronium ion interaction

The potential energy in the pore is assumed to only vary in the z-direction as shown in Eq. (A4); and hence, the sulfonate–hydronium ion potential energy is a function of z only. The modified Bessel function, K_0, and the term in the logarithm of Eq. (A4) are functions of (r, θ). We can eliminate the dependency on r and θ by integrating over the appropriate range of (r, θ); i.e., effectively averaging them over the pore's cross-sectional area. Thus, the total interaction potential energy, $V_{p\alpha}$, of the hydronium ions with the sulfonate groups within the pore element is

$$\begin{aligned} V_{p\alpha} &= \frac{q_1 q_2 N'_L}{\pi\varepsilon L}\iiint \rho_\alpha\Big(K(N_c, R, L_z) \\ &\quad\times \cos\left(2\pi N'_L\frac{z}{L}\right) - a(R)\Big)d\mathbf{x} \\ &= \iiint \rho_{m,\alpha}\frac{\Omega_s}{\varepsilon}\frac{F}{M_\alpha}\frac{2R}{N_c}\frac{N'_L}{N_L}\Big(K(N_c, R, L_z) \\ &\quad\times \cos\left(2\pi N'_L\frac{z}{L}\right) - a(R)\Big)d\mathbf{x}, \end{aligned} \tag{1}$$

where $K(N_c, R, L_z) = \frac{N_c}{\pi R^2}\int_0^R\int_0^{2\pi} K_0(2\pi\frac{r_{r\theta}}{L_z})d\theta r dr$ and $a(R) = \frac{N_c}{2\pi R^2}\int_0^R\int_0^{2\pi}\ln(r_{r\theta})d\theta r dr$.

2. Sulfonate–water interaction

The variation of the electric field due to the sulfonate groups is in the z direction and the dipole moment of the water molecules is oriented in the direction of the field. The electric field and total potential energy of the water molecules in the element is therefore expressed in terms of macroscopic variables according to

$$\begin{aligned} E_p(\mathbf{x}) &= -\frac{\partial\left(\frac{V_{p\alpha}}{\rho_{m,\alpha}}\frac{M_\alpha}{F}\right)}{\partial z} \\ &= \frac{\Omega_s}{\varepsilon}\frac{4\pi RN'_L}{N_c L}\frac{N'_L}{N_L}K(N_c, R, L_z)\sin\left(2\pi N'_L\frac{z}{L}\right) \end{aligned}$$

and

$$\begin{aligned} V_{ps} &= -\iiint N_s\mu E_p(\mathbf{x})d\mathbf{x} = -\iiint N_c(\lambda-1)\mu E_p(\mathbf{x})d\mathbf{x} \\ &= -\iiint \rho_{m,s}\frac{N_A}{M_s}\mu E_p(\mathbf{x})d\mathbf{x}, \end{aligned} \tag{2}$$

where $E_p(\mathbf{x})$ is the electric field at position $\mathbf{x}$ in the pore element, V_{ps} is the total potential energy in the pore element, μ is the dipole moment of a water molecule, and N_s is the total number of water molecules in the pore element, which is equal to $N_c \times (\lambda - 1)$.

3. Hydronium ion–hydronium ion interaction

The hydronium ions are assumed to be distributed randomly in the element of the pore. N_c hydronium ions constitute $\frac{N_c(N_c-1)}{2}$ pairs in the pore element. The average potential energy of a pair (e.g., i and j) of hydronium ions depends on the separation distance between them; i.e.,$|\mathbf{r}_{\alpha_i} - \mathbf{r}_{\alpha_j}|$ (given in Eq. (A5)). The total interaction potential energy of hydronium ions, $V_{\alpha\alpha}$, within the pore element is derived from the average potential energy of a pair and is expressed in terms of macroscopic variables as

$$\begin{aligned} V_{\alpha\alpha} &= \sum_{i>j=1}^{N_c}\frac{q_1^2}{4\pi\varepsilon|\mathbf{r}_{\alpha_i} - \mathbf{r}_{\alpha_j}|} \\ &= \frac{N_c(N_c-1)q_1^2}{8\pi\varepsilon}\left(\frac{1}{|\mathbf{r}_{\alpha_i} - \mathbf{r}_{\alpha_j}|}\right)_{\text{average}} \\ &= \frac{N_c(N_c-1)q_1^2}{8\pi\varepsilon}b_{\alpha\alpha} \\ &\approx \iiint\frac{\rho_{m,\alpha}^2 R^2 L_z}{8\varepsilon}\left(\frac{F}{M_\alpha}\right)^2 b_{\alpha\alpha}d\mathbf{x}, \end{aligned} \tag{3}$$

where $b_{\alpha\alpha} = (\frac{1}{|\mathbf{r}_{\alpha_i} - \mathbf{r}_{\alpha_j}|})_{\text{average}}$. Further details concerning this transformation can be found in the dissertation of Kumar.[18]

4. Hydronium ion–water molecule interaction

The total potential energy, $V_{\alpha s}$, within the pore element due to the hydronium ion–water interaction, using Eq. (A7), is expressed in terms of macroscopic variables $\rho_{m,\alpha}$ and $\rho_{m,s}$ as

$$\begin{aligned} V_{\alpha s} &= -\sum_{\alpha,i=1}^{N_c, N_s}\frac{\mu^2 q_1^2}{48\pi^2\varepsilon^2 k_B T|\mathbf{r}_\alpha - \mathbf{r}_s|^4} \\ &= -\frac{\mu^2 q_1^2 N_c}{48\pi^2\varepsilon^2 k_B T}\sum_{i=1}^{N_s}\frac{1}{|\mathbf{r}_\alpha - \mathbf{r}_s|^4} \\ &\approx -\frac{\mu^2 q_1^2 N_c N_s}{48\pi^2\varepsilon^2 k_B T}\left(\frac{1}{|\mathbf{r}_\alpha - \mathbf{r}_s|^4}\right)_{\text{average}} \\ &= -\iiint\rho_{m,\alpha}\rho_{m,s}\frac{N_A}{M_\alpha M_s}\frac{R^2 L_z\mu^2 F^2}{48\pi\varepsilon^2 R_g T}b_{\alpha s}d\mathbf{x}, \end{aligned} \tag{4}$$

where $b_{\alpha s} = (\frac{1}{|\mathbf{r}_\alpha - \mathbf{r}_s|^4})_{\text{average}}$ and the reader is again referred to Ref. 18.

5. Water–water interaction

There are $\frac{N_s(N_s-1)}{2}$ pairs of water molecules within the pore element. The average potential energy of a pair of water molecules depends on the separation distance between them; i.e., $|\mathbf{r}_{s_i} - \mathbf{r}_{s_j}|$, as given by Eq. (A6). The total interaction potential energy of water molecules, V_{ss}, in the pore element is derived from the average potential energy of a pair as

$$\begin{aligned} V_{ss} &= -\sum_{i>j=1}^{N_s} \frac{2\mu^4}{3(4\pi\varepsilon)^2 k_B T |r_i - r_j|^6} \\ &= -\frac{\mu^4 N_s(N_s-1)}{48\pi^2\varepsilon^2 k_B T}\left(\frac{1}{|r_{s_1} - r_{s_2}|^6}\right)_{\text{average}} \\ &\approx -\iiint \rho_{m,s}^2 \frac{N_A^3}{M_s^2}\frac{\mu^4 R^2 L_z}{48\pi\varepsilon^2 R_g T} b_{ss} d\mathbf{x}, \end{aligned} \tag{5}$$

where $b_{ss} = (\frac{1}{|\mathbf{r}_{s_i} - \mathbf{r}_{s_j}|^6})_{\text{average}}$.

6. Interaction with the external electric field

The external field, $E_{ext}(\mathbf{x})$, is applied in the z direction, as described by Qiao and Aluru.[19] The potential energy due to this applied external field at any point inside the pore may be written in terms of the macroscopic variables as

$$\begin{aligned} V_{ext,\alpha} &= \iiint \rho_{m,\alpha}\frac{F}{M_\alpha} V_{ext}(\mathbf{x}) d\mathbf{x}, \\ V_{ext,s} &= -\iiint \rho_{m,s}\frac{N_A}{M_s}\mu E_{ext}(\mathbf{x}) d\mathbf{x}, \end{aligned} \tag{6}$$

where $V_{ext}(\mathbf{x})$ is the applied potential and $V_{ext,\alpha}$ and $V_{ext,s}$ are the total potential energies of the hydronium ions and water molecules, respectively, in the pore element due to the external electric field.

B. Formulation of the generalized chemical potentials of the species

The Hamiltonian in the pore element is expressed as the sum of the kinetic energies of the species in the pore and their macroscopic interaction potential energies according to

$$\begin{aligned} &H[\rho_{m,\alpha},\ \rho_{m,s},\ \Pi_\alpha,\ \Pi_s] \\ &= \iiint \left(\frac{1}{2}\frac{\Pi_\alpha^2}{\rho_{m,\alpha}} + \frac{1}{2}\frac{\Pi_s^2}{\rho_{m,s}}\right) d\mathbf{x} \\ &\quad + V_{\alpha\alpha}(\rho_{m,\alpha}) + V_{\alpha s}(\rho_{m,\alpha},\ \rho_{m,s}) + V_{ss}(\rho_{m,s}) \\ &\quad + V_{p\alpha}(\rho_{m,\alpha}) + V_{ps}(\ \rho_{m,s}) + V_{ext,\alpha}(\rho_{m,\alpha}) + V_{ext,s}(\rho_{m,s}). \end{aligned} \tag{7}$$

The momentum density of a species i is related to the mass density and velocity of the species, $\mathbf{u}_i$, by $\Pi_i(\mathbf{x}) = \rho_{m,i}(\mathbf{x})\,\mathbf{u}_i(\mathbf{x})$. The generalized chemical potential of each species, μ_i^g, and its functional derivatives can be deduced from the above expression for the Hamiltonian[16]

$$\begin{aligned} \mu_\alpha^g &= \frac{\delta H}{\delta \rho_{m,\alpha}} \\ &= -\frac{u_\alpha^2}{2} + \frac{\rho_{m,\alpha} R^2 L F^2 b_{\alpha\alpha}}{4 M_\alpha^2 \varepsilon N_L'} - \frac{\rho_{m,s} N_A R^2 L \mu^2 F^2 b_{\alpha s}}{48 M_s M_\alpha \pi \varepsilon^2 R_g T N_L'} \\ &\quad + \frac{\Omega_s}{\varepsilon}\frac{F}{M_\alpha}\frac{2R}{N_c}\frac{N_L'}{N_L}\Big(K(N_c, R, L_z) \\ &\quad \times \cos\left(2\pi N_L'\frac{z}{L}\right) - a(R)\Big) + \frac{F V_{ext}}{M_\alpha}, \end{aligned} \tag{8}$$

$$\begin{aligned} \mu_s^g &= \frac{\delta H}{\delta \rho_{m,s}} \\ &= -\frac{u_s^2}{2} - \frac{\rho_{m,\alpha} N_A R^2 L \mu^2 F^2 b_{\alpha s}}{48 M_\alpha M_s \pi \varepsilon^2 R_g T N_L'} - \frac{\rho_{m,s}\mu^4 R^2 L N_A^3 b_{ss}}{24 M_s^2 \pi \varepsilon^2 R_g T N_L'} \\ &\quad - \frac{\Omega_s \mu}{\varepsilon}\frac{N_A 4\pi N_L' R}{M_s N_c L}\frac{N_L'}{N_L} K(N_c, R, L_z)\sin\left(2\pi N_L'\frac{z}{L}\right) \\ &\quad - \frac{N_A \mu E_{ext,z}}{M_s}. \end{aligned} \tag{9}$$

C. Derivation of the evolution equations via nonequilibrium thermodynamics

The derivation of the equations of motion uses the bracket methodology of nonequilibrium thermodynamics.[16,20] This methodology allows the consistent, physical derivation of equations of motion for complicated systems wherein many different physical processes are interacting by employing a rigorous mathematical framework common to all dynamical phenomena. This structure is embedded into two complementary bracket structures: the Poisson bracket of traditional classical mechanics, accounting for conservative, reversible processes, and the dissipation bracket, which accounts for irreversible phenomena. The structure of these brackets ensures that all required thermodynamic principles are incorporated into the final set of evolution equations for the system variables, while maintaining the integrity of the physical interactions between multiple dynamical system processes.[16]

For the present case, we assume constant temperature and define the relevant Poisson and dissipation brackets for a two-component system expressed in terms of an arbitrary functional of the system variables, F, and the Hamiltonian, Eq. (7), as[16]

$$\begin{aligned} \{F, H\} = &-\sum_{i=1}^{2}\iiint\left[\frac{\delta F}{\delta\rho_{m,i}}\nabla\cdot\left(\frac{\delta H}{\delta \mathbf{u}_i}\rho_{m,i}\right)\right. \\ &\left. - \frac{\delta H}{\delta\rho_i}\nabla\cdot\left(\frac{\delta F}{\delta \mathbf{u}_i}\rho_{m,i}\right)\right] d\mathbf{x} \\ &- \sum_{i=1}^{2}\left[\iiint\frac{\delta F}{\delta \mathbf{u}_i}\nabla\cdot\left(\frac{\delta H}{\delta \mathbf{u}_i}\mathbf{u}_i\right)\right. \\ &\left. - \frac{\delta H}{\delta \mathbf{u}_i}\nabla\cdot\left(\frac{\delta F}{\delta \mathbf{u}_i}\mathbf{u}_i\right)\right] d\mathbf{x}, \end{aligned} \tag{10}$$

$$[F,H] = -\sum_{i=1}^{2}\iiint \kappa_i \left[\nabla\left(\frac{\delta F}{\delta \mathbf{u}_i}\right) : \nabla\left(\frac{\delta H}{\delta \mathbf{u}_i}\right) + \nabla\left(\frac{\delta H}{\delta \mathbf{u}_i}\right) : \nabla\left(\frac{\delta F}{\delta \mathbf{u}_i}\right)\right] d\mathbf{x} - \sum_{i=1}^{2}\iiint D_{\mu_i}\nabla\left(\frac{\delta F}{\delta \rho_{m,i}}\right)\cdot\nabla\left(\frac{\delta H}{\delta \rho_{m,i}}\right) d\mathbf{x}, \quad (11)$$

where i is either α or s and the ∇ represents the gradient operator. In these expressions, H is the Hamiltonian of Eq. (7) and F is an arbitrary functional of the same variables as H. The symbols D_{μ_i} and κ_i relate to the diffusivities of the species and their viscosities, respectively, as defined in Subsection II D. The equations of motion for the problem variables are then obtained from the dynamical equation of change for the functional, F, expressed as

$$\frac{dF}{dt} = \{F,H\} + [F,H]. \quad (12)$$

The equations of change for the system variables can then be derived from this expression as Eq. (13). The details of this derivation are provided in the dissertation of Kumar.[18]

D. Transport of hydronium ions and water molecules

In this work, we consider transport in the z direction only. Hence, the full system of evolution equations in 3-dimensions (which may be found in Ref. 18) reduce to four coupled equations for mass and momentum transport of the species based on their chemical potentials:

$$\frac{\partial \rho_{m,i}}{\partial t} = -\frac{\partial(u_i\rho_{m,i})}{\partial z} + D_{\mu_i}\frac{\partial^2 \mu_i^g}{\partial z^2}$$

$$\rho_{m,i}\frac{\partial u_i}{\partial t} = -\rho_{m,i}u_{i,z}\frac{\partial u_i}{\partial z} - \rho_{m,i}\frac{\partial \mu_i}{\partial z} + \eta\frac{\partial^2 u_i}{\partial z^2}, \quad (13)$$

where u_i is the velocity component in the z direction of species i. The generalized chemical potentials of the species, μ_i^g, are defined by Eqs. (8) and (9) and are equal to $\mu_i - \frac{1}{2}u_i^2$, where μ_i is the chemical potential of the species i. The symbols D_{μ_i} and κ_i represent the diffusivities of the species and their viscosities, respectively. (Note: $2\kappa_\alpha = 2\kappa_s = \eta$, the viscosity of water.)

D_{μ_i} is the diffusion coefficient based on the chemical potential of the species. This can be related to the diffusion coefficient based on the number density (D_{ρ_i}) of the species by $D_{\mu_i} = \frac{D_{\rho_i}M_i\bar{\rho}_{m,i}}{R_gT}$, where $\bar{\rho}_{m,i}$ is the average mass density of the species in the pore. Whereas D_{ρ_i} is an implicit function of the concentration of the species and varies inversely to $\bar{\rho}_{m,i}$,[21] $D_{\rho_i}\bar{\rho}_{m,i}$ can be assumed constant, which implies D_{μ_i} is also a constant at a specified temperature. The mass densities of the species, $\rho_{m,i}$, are used to derive their number densities according to $\rho_i = \frac{\rho_{m,i}}{M_i}N_A$. Equations (13) can be rewritten in terms of the number densities of the species as

$$\frac{\partial \rho_i}{\partial t} = -\frac{\partial(u_i\rho_i)}{\partial z} + \frac{D_{\rho_i}M_i}{R_gT}\bar{\rho}_i\frac{\partial^2 \mu_i^g}{\partial z^2}$$

$$\rho_i\frac{\partial u_i}{\partial t} = -\rho_i u_i\frac{\partial u_i}{\partial z} - \rho_i\frac{\partial \mu_i^g}{\partial z} + \frac{\eta N_A}{M_i}\frac{\partial^2 u_i}{\partial z^2}. \quad (14)$$

The chemical potentials and their derivatives are substituted into the above equations and rendered dimensionless using to following definitions: $\tilde{t} = \frac{tV_{av}}{L}$, $\tilde{z} = \frac{z}{L}$, $\tilde{u}_i = \frac{u_i}{V_{av}}$, and $\tilde{\rho}_i = \frac{\rho_i}{\bar{\rho}_i}$, where V_{av} is the average velocity of the species if the surface charge on the pore wall is zero and $\bar{\rho}_i$ is the average number density of species i in the pore. The resulting transport equations (number density and velocity) for the hydronium ions are

$$\frac{\partial \tilde{\rho}_\alpha}{\partial \tilde{t}} = -\frac{\partial(\tilde{u}_\alpha\tilde{\rho}_\alpha)}{\partial \tilde{z}} - Di_\alpha\left[\tilde{u}_\alpha\frac{\partial^2\tilde{u}_\alpha}{\partial\tilde{z}^2} + \left(\frac{\partial\tilde{u}_\alpha}{\partial\tilde{z}}\right)^2\right] + Di_\alpha Hh_\alpha\frac{\partial^2\tilde{\rho}_\alpha}{\partial\tilde{z}^2} + Di_\alpha Hy_\alpha\frac{\partial^2\tilde{\rho}_s}{\partial\tilde{z}^2} - Di_\alpha Me_\alpha(\pi N_L')K(N_c,R,L_z)\cos(2\pi N_L'\tilde{z}), \quad (15)$$

$$Re_\alpha\tilde{\rho}_\alpha\frac{\partial\tilde{u}_\alpha}{\partial\tilde{t}} = -Re_\alpha\tilde{\rho}_\alpha\tilde{u}_\alpha\frac{\partial\tilde{u}_\alpha}{\partial\tilde{z}} - Re_\alpha Hh_\alpha\tilde{\rho}_\alpha\frac{\partial\tilde{\rho}_\alpha}{\partial\tilde{z}} - Re_\alpha Hy_\alpha\tilde{\rho}_\alpha\frac{\partial\tilde{\rho}_s}{\partial\tilde{z}} + \frac{Re_\alpha Me_\alpha}{2}\tilde{\rho}_\alpha K(N_c,R,L_z)\sin(2\pi N_L'\tilde{z}) + Re_\alpha En_\alpha\tilde{\rho}_\alpha + \frac{d}{L}\frac{\partial^2\tilde{u}_\alpha}{\partial\tilde{z}^2}, \quad (16)$$

where $Di_\alpha = \frac{D_{\rho\alpha}M_\alpha}{R_gT}\frac{V_{av}}{L}$, $Hh_\alpha = \frac{\bar{\rho}_\alpha R^2LF^2b_{\alpha\alpha}}{4M_\alpha N_A{V_{av}}^2\varepsilon N_L'}$, $Hy_\alpha = -\frac{\bar{\rho}_s R^2L\mu^2F^2b_{\alpha s}}{48M_\alpha\pi\varepsilon^2R_gTN_L'{V_{av}}^2}$, $Me_\alpha = \frac{\Omega_s RF}{M_\alpha\varepsilon{V_{av}}^2}\left(\frac{8\pi N_L'^2}{N_cN_L}\right)$, $Re_\alpha = \frac{\bar{\rho}_\alpha M_\alpha dV_{av}}{\eta N_A}$, $En_\alpha = \frac{FE_{ext}L}{M_\alpha{V_{av}}^2}$, and d is the diameter of the tube. Similarly, the transport equations (number density and velocity) for the water molecules are

$$\frac{\partial\tilde{\rho}_s}{\partial\tilde{t}} = -\frac{\partial(\tilde{u}_s\tilde{\rho}_s)}{\partial\tilde{z}} - Di_s\left[\tilde{u}_s\frac{\partial^2\tilde{u}_s}{\partial\tilde{z}^2} + \left(\frac{\partial\tilde{u}_s}{\partial\tilde{z}}\right)^2\right] + Di_sHy_s\frac{\partial^2\tilde{\rho}_\alpha}{\partial\tilde{z}^2} + Di_sWa_s\frac{\partial^2\tilde{\rho}_s}{\partial\tilde{z}^2} + Di_sMe_s(2\pi^2N_L'^2)K(N_c,R,L_z)\sin(2\pi N_L'\tilde{z}), \quad (17)$$

$$Re_s\tilde{\rho}_s\frac{\partial\tilde{u}_s}{\partial\tilde{t}} = -Re_s\tilde{\rho}_s\tilde{u}_s\frac{\partial\tilde{u}_s}{\partial\tilde{z}} - Re_sHy_s\tilde{\rho}_s\frac{\partial\tilde{\rho}_\alpha}{\partial\tilde{z}} - Re_sWa_s\tilde{\rho}_s\frac{\partial\tilde{\rho}_s}{\partial\tilde{z}} + Re_sMe_s(\pi N_L')\tilde{\rho}_sK(N_c,R,L_z)\cos(2\pi N_L'\tilde{z}) + \frac{d}{L}\frac{\partial^2\tilde{u}_s}{\partial\tilde{z}^2}, \quad (18)$$

where $Di_s = \frac{D_{\rho s}M_s}{R_gT}\frac{V_{av}}{L}$, $Hy_s = -\frac{\bar{\rho}_\alpha R^2L\mu^2F^2b_{\alpha s}}{48M_s\pi\varepsilon^2R_gTN_L'{V_{av}}^2}$, $Wa_s = -\frac{\bar{\rho}_sR^2LN_A^2\mu^4b_{ss}}{24M_s\pi\varepsilon^2R_gTN_L'{V_{av}}^2}$, $Me_s = \frac{\Omega_sR\mu N_A}{M_s\varepsilon{V_{av}}^2L}\left(\frac{8\pi N_L'^2}{N_cN_L}\right)$, and $\mathrm{Re}_s = \frac{\bar{\rho}_sM_sdV_{av}}{\eta N_A}$.

The dimensionless groups appearing above are ratios of the relative strengths of the various forces acting within the system. For example, Re_i is the familiar Reynolds number of fluid mechanics, which represents the ratio of inertial to

viscous forces. The reader is referred to the dissertation of Kumar for further details.[18] Altogether, these equations describe the variations of the species densities and velocities (averaged over the pore area) along the length of the pore, which can be used to calculate the flux and the proton conductivity within the pore.

E. Analytical solution of the transport equations

The interface is very thin compared to the membrane and hence we assume that the density of water molecules is uniform along the pore length ($\tilde{\rho}_s = \text{constant}$) and that the water is stationary at the continuum level ($\tilde{u}_s = 0$). The above transport equations for hydronium ions were solved analytically at steady state using an order-of-magnitude analysis. The approximation of the terms in the transport equations was performed by using the appropriate values of the dimensionless groups and physical constants, as determined by experiment and fundamental theory, as well as by evaluating and comparing the relative values of the dimensionless groups. The values of all parameters and constants used in the model are summarized in Appendix B.

1. Density variation within the pore

The magnitude of all terms in the transport equations can be estimated by using the values of the dimensionless parameters Di_α, Hh_α, Hy_α, Me_α, Re_α, and En_α. At steady state, the first and second terms on the right side of Eq. (15) are negligible in magnitude in comparison to the rest of the terms. The density of water is assumed to be constant; i.e., the fourth term is zero. The non-dimensional density of hydronium ions can be derived by integrating this equation and can be written as

$$\tilde{\rho}_\alpha = -\frac{Me_\alpha K(N_c, R, L_z)}{Hh_\alpha(4\pi N_L')}\cos(2\pi N_L'\tilde{z}) + a\tilde{z} + b, \qquad (19)$$

where a and b are constants of integration.

Two boundary conditions are required to determine these constants. We assumed that the density gradient at the entrance of the pore is zero (the flux of the hydronium ions at the entrance is due to the gradient in its chemical potential) and, as a result, $a = 0$. A pore is electrically neutral; therefore, the total number of hydronium ions should always be equal to the number of sulfonate ions within the pore. The integration of the density function of Eq. (19) along the pore length results in a unit value; i.e., $b = 1$. Thus, the density variation of the hydronium ions can be expressed as

$$\tilde{\rho}_\alpha = 1 - \frac{Me_\alpha K(N_c, R, L_z)}{Hh_\alpha(4\pi N_L')}\cos(2\pi N_L'\tilde{z}), \qquad (20)$$

which shows that the density varies sinusoidally within the pore and depends on the concentration of sulfonate groups and hydronium ions, the separation distance between two consecutive rings of sulfonate groups, and the radius of the pore. This expression is similar to the expression of potential energy due to sulfonate groups on the pore wall [see Eq. (1)]. The magnitude of the average potential energy, $V_{p\alpha}$, is a maximum at the axial positions of the rings of sulfonate groups and is a minimum between any two adjacent rings. Thus, the hydronium ion density also varies according to the potential energy. Me_α, a negative quantity, is related to the interaction of sulfonate groups with the hydronium ions and is proportional to the surface charge density on the pore wall. Hy_α, a positive quantity, is related to the hydronium ion–hydronium ion interaction and is proportional to the hydronium ion density within the pore. These parameters also depend on the pore specifications: pore radius, distance between two consecutive rings, and number of sulfonate groups in a ring. The magnitude of the minimum and maximum density regions within the pore depends on the ratio of the magnitudes of Me_α and Hh_α; i.e., the surface charge density on the pore wall, Ω_s, and the density of hydronium ions, ρ_α. Increasing Ω_s increases the attractive force between sulfonate groups and hydronium ions and therefore hydronium ions accumulate near the rings. This causes a large difference between the maximum and minimum density regions within the pore. Increasing ρ_α augments the hydronium ion–hydronium ion interaction, and results in a relatively uniform density of hydronium ions within the pore.

2. Velocity variation within the pore

The expression of the density variation in Eq. (20) can be applied to Eq. (16) at the steady-state condition, yielding

$$0 = -Re_\alpha\tilde{\rho}_\alpha\tilde{u}_\alpha\frac{\partial\tilde{u}_\alpha}{\partial\tilde{z}} + Re_\alpha En_\alpha\tilde{\rho}_\alpha + \frac{d}{L}\frac{\partial^2\tilde{u}_\alpha}{\partial\tilde{z}^2}. \qquad (21)$$

The first term in Eq. (21) is ten orders of magnitude lower than the second term and seven orders of magnitude lower than the third term; hence, this term may be neglected. The non-dimensional velocity variation along the pore length can then be derived by integrating the above equation:

$$\tilde{u}_\alpha = -\frac{L}{d}Re_\alpha En_\alpha\left(\frac{\tilde{z}^2}{2} + \frac{Me_\alpha K(N_c, R, L_z)}{16Hh_\alpha(\pi N_L')^3}\cos(2\pi N_L'\tilde{z})\right) + A\tilde{z} + B, \qquad (22)$$

where A and B are constants of integration. Two boundary conditions are required to determine these constants. The velocity gradient (related to the constant, A) is unknown at the entrance of the pore; rather, we know that the flux of hydronium ions should be constant according to the mass conservation principle. (We will show in Subsection II E 3 that we do not need any information concerning A in order to calculate the flux and conductivity in the pore.) We take the average velocity at the entrance of the pore as $V_{av} = V_\alpha$, which is the steady-state velocity of the hydronium ions achieved under the effect of the external electric field; this can be determined using the Nernst-Einstein equation. Hence, $\tilde{u}_\alpha(\tilde{z} = 0) = 1$. The value of B can be determined as

$$B = 1 + \frac{L}{d}Re_\alpha En_\alpha\frac{Me_\alpha K(N_c, R, L_z)}{16Hh_\alpha(\pi N_L')^3}, \qquad (23)$$

and, accordingly, the dimensionless velocity of hydronium ions within the pore can be written as

$$\tilde{u}_\alpha = 1 + \frac{L}{d}Re_\alpha En_\alpha\frac{Me_\alpha K(N_c, R, L_z)}{16Hh_\alpha(\pi N_L')^3}(1 - \cos(2\pi N_L'\tilde{z})) - \frac{L}{d}Re_\alpha En_\alpha\frac{\tilde{z}^2}{2} + A\tilde{z}. \qquad (24)$$

This expression indicates that the velocity also varies sinusoidally in the pore and depends on the concentration of sulfonate and hydronium ions, separation distance between sulfonate groups, applied electric field, viscosity of the fluid, and length and radius of the pore. The nature of the velocity profile is a function of the velocity gradient, A, at the entrance of the pore. The mass conservation of hydronium ions requires that the flux of the hydronium ions within the pore should be constant in the axial direction. The velocity variation within the pore is out of phase with the number density variation. Thus, the velocity is a minimum where number density is a maximum; i.e., in the vicinity of the rings of sulfonate groups. Conversely, it is a maximum where the number density is a minimum; i.e., between the two rings. These deductions from Eq. (2) indicate that the hydronium ions are slowed down as they pass by the attractive sulfonate ions.

3. Calculation of the flux and conductivity within the pore

The number density and velocity of hydronium ions change sinusoidally within the pore, but the flux is constant along the pore length. The non-dimensional flux of hydronium ions in the pore can thus be calculated using the number density and velocity variations within the pore:

$$\tilde{\rho}_\alpha \tilde{u}_\alpha = \left[1 - \frac{Me_\alpha K(N_c, R, L_z)}{Hh_\alpha(4\pi N_L')} \cos(2\pi N_L' \tilde{z})\right] \times \left[1 + \frac{L}{d} Re_\alpha En_\alpha \frac{Me_\alpha K(N_c, R, L_z)}{16Hh_\alpha(\pi N_L')^3} \times (1 - \cos(2\pi N_L' \tilde{z})) - \frac{L}{d} Re_\alpha En_\alpha \frac{\tilde{z}^2}{2} + A\tilde{z}\right], \quad (25)$$

which is a function of axial position, z. However, the constant flux constraint eliminates the z variation of the flux in Eq. (25), and hence,

$$\tilde{\rho}_\alpha \tilde{u}_\alpha = 1 + \frac{L}{d} Re_\alpha En_\alpha \frac{Me_\alpha K(N_c, R, L_z)}{16Hh_\alpha(\pi N_L')^3}. \quad (26)$$

This equation can be further simplified by replacing the non-dimensional parameters by their respective definitions, giving

$$\tilde{\rho}_\alpha \tilde{u}_\alpha = 1 + \frac{2}{\pi^2 N_L N_c} \frac{\Omega_s}{F} \frac{L}{R} \frac{R_g T}{\eta D_{\rho_\alpha}} \frac{K(N_c, R, L_z)}{b_{\alpha\alpha}(N_c, R, L_z)}, \quad (27)$$

and, accordingly, the flux within the pore can be expressed as

$$\rho_\alpha u_\alpha = \bar{\rho}_\alpha V_\alpha \left(1 + \frac{2}{\pi^2 N_L N_c} \frac{\Omega_s}{F} \frac{L}{R} \frac{R_g T}{\eta D_{\rho_\alpha}} \frac{K(N_c, R, L_z)}{b_{\alpha\alpha}(N_c, R, L_z)}\right). \quad (28)$$

The above equation shows that the flux is constant within the pore and its magnitude depends on the pore specifications, fluid properties, and external field. The multiplier $\bar{\rho}_\alpha V_\alpha$ in the above expression is the flux of hydronium ions through the pore as if there were no sulfonate groups on the pore wall. The second term in this equation is negative because the surface charge density on the wall, Ω_s, is negative, which shows that the introduction of surface charges on the pore wall decreases the flux of hydronium ions through the pore. The parameters $K(N_c, R, L_z)$ and $b_{\alpha\alpha}(N_c, R, L_z)$ represent the interactions of hydronium ions with sulfonate ions and hydronium ion–hydronium ion interactions, respectively, within the pore element, and depend on the radius of the pore, number of sulfonate groups in a ring on the circumference (at constant axial position), and the separation distance between two consecutive rings of sulfonate groups. These parameters also appeared in Eqs. (1) and (3), respectively, and can be calculated with the knowledge of pore specifications.

The flux of the hydronium ions within the pore is directly related to the current density, j, by

$$j = \rho_\alpha u_\alpha \frac{F}{N_A}. \quad (29)$$

The proton conductivity of the pore is related to the current density and external electric field in the pore by the expression

$$\sigma = \frac{j}{|E_{ext}|}. \quad (30)$$

Substituting Eqs. (28) and (29) into Eq. (30), the conductivity of the pore is determined as

$$\sigma = \sigma_0 \left(1 + \frac{2}{\pi^2 N_L N_c} \frac{\Omega_s}{F} \frac{L}{R} \frac{R_g T}{\eta D_{\rho_\alpha}} \frac{K(N_c, R, L_z)}{b_{\alpha\alpha}(N_c, R, L_z)}\right), \quad (31)$$

where

$$\sigma_0 = \frac{D_{\rho_\alpha}}{R_g T} F^2 \frac{\bar{\rho}_\alpha}{N_A}. \quad (32)$$

Equation (32) represents the conductivity of the pore as if there were no sulfonate groups present. The sulfonate anions on the wall reduce the conductivity, and hence its value depends on the morphology of the interface. Using the definition of surface charge density of Eq. (31), the conductivity expression can further be simplified to

$$\sigma = \sigma_0 \left(1 - \frac{2}{\pi^2 R^2} \frac{k_B T}{\eta D_{\rho_\alpha}} \frac{K(N_c, R, L_z)}{b_{\alpha\alpha}(N_c, R, L_z)}\right), \quad (33)$$

which quantifies the reduction in the conductivity due to the presence of sulfonate ions on the pore wall. The parameters K and $b_{\alpha\alpha}$ depend on the number of sulfonate groups in a ring, the pore radius, and the separation distance between two consecutive rings.

In the above expressions of the conductivity, the diffusion constant of hydronium ions in the membrane water, D_{ρ_α}, is a function of water content. This can be related to the diffusion coefficient of hydronium ions in bulk water, $D_{\alpha s}$, and porosity and tortuosity of the membrane by

$$D_{\rho_\alpha} = \frac{\varepsilon_w}{\tau} D_{\alpha s}, \quad (34)$$

where ε_w and τ are the porosity and tortuosity of the membrane, respectively. The porosity and tortuosity depend on the internal structure and water content of the membrane. The effective tortuosity can be introduced by replacing Eq. (34) by[9]

$$D_{\rho_\alpha} = K_1 D_{\alpha s}, \quad (35)$$

where

$$K_1 = (\varepsilon_w - \varepsilon_{w0})^q , \tag{36}$$

ε_w and ε_{w0} are the porosities of the membrane at water contents λ and λ_0, respectively. λ_0 is the minimum water content of the membrane below which proton diffusion does not occur in the membrane due to lack of connectivity of the water phase. Consequently, ε_{w0} may be referred to as the threshold porosity, and $(\varepsilon_w - \varepsilon_{w0})$ is the volume fraction of the water phase through which diffusion is occurring.[9,22] The value of the Bruggeman exponent typically used is $q = 1.5$;[9,23] it is sometimes used as a fitting parameter. The porosity of the membrane can be related to the partial molar volumes of a dry membrane and water by[9]

$$\varepsilon_w = \frac{\lambda}{\lambda + \bar{V}_m/\bar{V}_s}, \tag{37}$$

where $\bar{V}_m$ and $\bar{V}_s$ are the partial molar volumes of the dry membrane and water, respectively. The molar volume of dry membrane can be approximated as the ratio of equivalent weight of the membrane and density of the dry membrane:[9]

$$V_m \approx \frac{\mathrm{EW}}{\rho_m}, \tag{38}$$

where EW is the equivalent weight of the membrane and is defined as the ratio of the weight of dry membrane in grams to the moles of acid groups in the membrane. Also, ρ_m is the density of the dry membrane. For a Nafion 117 membrane, EW = 1100 g/mol and ρ_m = 2.05 g/cm;[9] thus, $\bar{V}_m$ = 536.6 cm^3/mol. The partial molar volume of water, $\bar{V}_s$, is 18.016 cm^3/mol. The value of minimum water content, λ_0, is taken as 1.9 to calculate the threshold porosity of the membrane.[9,24]

The size of a hydronium ion is almost the same as that of a water molecule; hence, they can be treated as identical particles. The Stokes-Einstein equation for the self-diffusion coefficient of identical particles assumes the complete slip condition,[21] and the expression of the self-diffusion is

$$D_{\alpha s} = \frac{k_B T}{\eta 2\pi}\left(\frac{N_A}{\bar{V}_s}\right)^{1/3}, \tag{39}$$

where $D_{\alpha s}$ is quantified by Eqs. (34) and (35). Subsections III A–III E discuss the effect of radius, water content, and sulfonate distribution over the pore wall on the conductivity.

III. RESULTS AND DISCUSSION

The expression of Eq. (33) shows that proton conductivity depends on the morphology of the interface. Factors comprising the morphology include the pore size (length and radius), number of sulfonate groups on the pore wall, tortuosity, and porosity of the interfacial region. The parameter $K(N_c, R, L_z)$ quantifies the interaction of hydronium ions with sulfonate ions on the pore wall and $b_{\alpha\alpha}(N_c, R, L_z)$ scales the hydronium ion–hydronium ion interactions, as expressed by Eqs. (1) and (3), respectively. These parameters depend on the radius and length of the pore as well as the concentration of hydronium ions within the pore. It is evident from Eq. (33) that the conductivity decreases with increasing sulfonate–hydronium interactions (K in the numerator) and increases with increasing hydronium–hydronium interactions ($b_{\alpha\alpha}$ in the denominator). The effect of all the above factors on the proton conductivity of a pore is discussed in Subsections III A–III E.

A. Effect of water content and pore radius on conductivity

To examine the effect of water content and radius on the conductivity, we considered two pores of radii 8 and 10 Å, each at three water contents, 6, 12, and 18. The total number of sulfonate groups in the pores was 36; i.e., $N_L \times N_c = 36$. We also assumed that the pores were filled with water; thus, the volume is directly proportional to the number of water molecules within the pore, $N_L \times N_c \times \lambda$. Accordingly, the volumes of the pores at the same water content are equivalent, and the pore of higher radius will be smaller in length. The number of hydronium ions in a pore is equal to the number of sulfonate ions, which is fixed in this case; thus, the concentration of hydronium ions in all pores is the same.

The conductivities of these pores, calculated using Eq. (33), are presented in Table I. The sulfonate distribution is $N_L = 9$ and $N_c = 4$. The last column in Table I represents the experimental conductivity data for a Nafion membrane at the specified water contents.[25] The results reveal that the calculated conductivities are reasonably close to the experimental values. L_r in Table I is the distance between two consecutive sulfonate groups in a ring and L_s is the average separation distance between two sulfonate groups on the pore wall. These distances can be expressed as

$$L_r = \frac{2\pi R}{N_c}, \tag{40}$$

$$L_s = \frac{N_L' L_z + N_c L_r}{N_L' + N_c}. \tag{41}$$

Increasing the number of sulfonate groups, N_c, in the ring decreases L_r; thus, the smaller value of L_r results in the stronger local attractive force between SO_3^- groups and H_3O^+ ions. This force restricts the motion of the hydronium ions along the pore length, thereby decreasing proton conductivity. If two

TABLE I. Conductivity (σ) variation with water content (λ) and pore radius (R). Total number of sulfonate groups in the pore is $N_L \times N_c = 36$, where N_L and N_c are number of rings of sulfonate groups along the length and number of sulfonate groups in a ring, respectively; these are 9 and 4, respectively. The volumes of two pores at the same values of λ are equivalent. L_z, L_r, and L_s are the separation distance between two consecutive rings, between two consecutive sulfonate groups in a ring, and the average separation distance between two sulfonate groups on the pore wall, respectively. Calculated conductivities are quantitatively similar to the experimental data.

	$R = 8$ Å				$R = 10$ Å				Expt.
λ (#H_2O/–SO_3H)	L_z (Å)	L_r (Å)	L_s (Å)	σ (S/cm)	L_z (Å)	L_r (Å)	L_s (Å)	σ (S/cm)	σ[a] (S/cm)
6	4.0	12.6	6.9	0.0265	2.6	15.7	7.0	0.0287	0.02
12	8.0	12.6	9.5	0.0401	5.1	15.7	8.7	0.0437	0.05
18	12.0	12.6	12.2	0.0423	7.7	15.7	10.4	0.0477	0.06

[a]Experimental proton conductivity data for a Nafion membrane at room temperature.[25]

pores have the same value of N_c, the lower radius pore will have a lower value of L_r, and the interaction distance between the sulfonate groups and hydronium ions is thus lower; the result is a stronger attractive force. The lower value of $L_r$in the pore decreases the proton conductivity. On the other hand, L_z is the separation distance between two consecutive rings of sulfonate groups, and its magnitude determines the relative dominance of sulfonate–hydronium ion and hydronium ion–hydronium ion interactions. The smaller value of L_z results in higher conductivity as the hydronium ions move more freely from one ring to the next due to the inductive attraction down the axial length of the pore. Smaller L_z also decreases the interaction distance between the hydronium ions, thus resulting in a higher value of $b_{\alpha\alpha}$.

Table I also shows that the conductivities of the pores of radius 10 Å are higher than those of the corresponding 8 Å pores. The volumes of the pores at a specified water content are the same; thus, the length of the pore of radius 10 Å is smaller. In other words, L_z is smaller for this pore at a specified sulfonate distribution scheme. A larger radius also implies a higher value of L_r. Both of these (lower L_z and higher L_r) result in higher conductivity. Physically, as the pore radius increases, the hydronium ions are, on average, farther away from the sulfonate charges on the wall, and hence can move more freely through the pore.

In general, a pore expands with increasing water content. If two pores have the same radius, the pore with the higher water content will be longer. As a result, L_r is same for all pores, but L_z increases with increasing water content. This decreases the net attraction of hydronium ions from one ring to the next and, thus, decreases the conductivity. On the other hand, increasing water content also decreases the ratio of interaction parameters K and $b_{\alpha\alpha}$, which increases the conductivity according to Eq. (33). In this case, the combined effect of these two factors results in the increase of the conductivity with increasing water content.

B. Effect of sulfonate distribution on proton conductivity

In Sec. III A, our results showed that increasing water content increases the conductivity; however, the sulfonate distribution over the pore wall exhibited a strong effect on the conductivity. Figure 2(a) shows the variation of proton conductivity with increasing water content for three sulfonate distribution schemes. All pores have a radius 8 Å and the total number of sulfonate groups on the pore wall is 36. The lengths of the pores and, thus, the correspondingL_z values, depend on the water content, as discussed in Sec. III A. Figure 2(b) shows the dependency of L_z on water content and sulfonate distribution. These figures show that conductivity strongly depends on distance between two rings of sulfonate groups, L_z. As the number of sulfonate groups in the pores is constant, increasing N_c decreases N_L; consequently, L_z increases. This results in a stronger local force of sulfonate rings with hydronium ions and an accumulation of hydronium ions in the vicinity of rings; therefore, there is less conduction of hydronium ions down the pore because adjacent rings are further apart. As a consequence, the average flux of hydronium

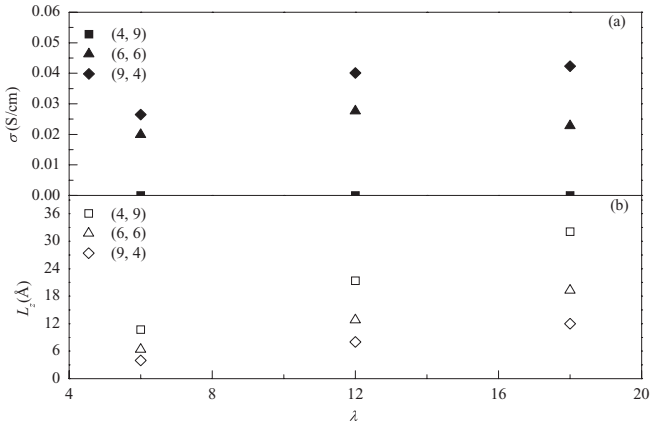

FIG. 2. Variation of (a) conductivity (σ) and (b) L_z with water content (λ) and sulfonate distribution(N_L, N_c), where N_L and N_c are the number of rings of sulfonate groups along the length and number of sulfonate groups in a ring, respectively. L_z is the separation distance between two consecutive rings of charges along the pore length. The pore is of radius 8 Å and the total number of sulfonate groups on the pore wall is 36. Three distribution schemes were considered. The pore is filled with water and the volume of a pore is directly proportional to its water content.

ions along the pore is very low. The figure also shows that the conductivity for sulfonate distribution of (4, 9) is almost zero, even at higher water contents, because the large number of sulfonate charges in a ring produces a highly attractive environment for the hydronium ions. Furthermore, higher water contents require higher values of L_z, which increases from 10.7 to 32.1 Å on increasing water content from 6 to 18. For (6,6), conductivity increases with increasing water content from 6 to 12, but after that it decreases because of higher values of L_z. For (9, 4), conductivity increases with increasing water content, but higher water content has less effect on the conductivity because of the increasing value of L_z. This shows that the sulfonate distribution along with separation distance plays an important role in the proton conduction.

C. Conductivity of pore with $N_T = 72$

In this subsection, we studied the conductivity of pores with total number of sulfonate groups, $N_T = 72$, twice the number of the previous case. The volume of a water-filled pore is directly proportional to $N_L \times N_c \times \lambda$. If two pores have the same water content, the pore with the higher number of sulfonate ions has a larger volume; i.e., the volume of a pore with $N_L \times N_c = 72$ and $\lambda = 6$ will be twice that of a pore with $N_L \times N_c = 36$ and $\lambda = 6$.

The conductivities of the pores of radii 10, 12, and 14 Å at water contents 6, 12, and 18 are shown in Fig. 3. Four sulfonate distribution schemes were considered: (6, 12), (8, 9), (9, 8), and (12, 6). The numerical values in the legend are (N_L, N_c, R). For pores of larger radius, the conductivity increases with water content for all distributions; however, it decreases as the distribution shifts to higher N_c and lower N_L, as noted in Subsection III B. Again, this is because the larger number of sulfonate groups in the rings provides a stronger local attraction that hinders the transport of the hydronium ions down the tube. Furthermore, as the number of rings decreases, the distance between them, L_z, increases, thus dampening the

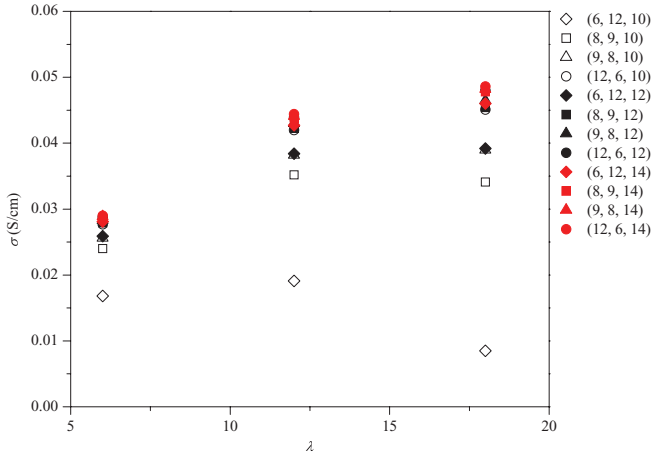

FIG. 3. Variation of conductivity (σ) with water content (λ), sulfonate distribution (N_L, N_c), and pore radius (R). The numerical values in the legends are (N_L, N_c, λ). The total number of sulfonate groups on the pore wall is 72.

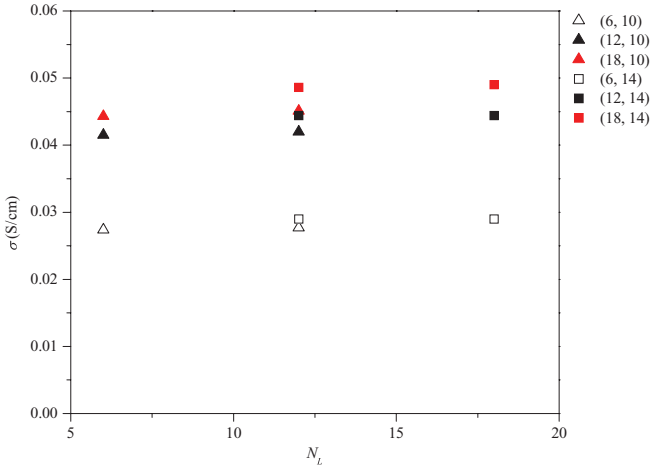

FIG. 5. Variation of conductivity (σ) with number of rings of sulfonate groups (N_L). The numerical values in the legends are (λ, R). The number of sulfonate groups in each ring (N_c) is 6.

transit of hydronium ions from one ring to the next. For pores of smaller radius, the conductivity actually decreases at high water contents, especially at high values of N_c. This is because the attractive force between the ring sulfonate groups and the hydronium ions is much higher on average at small radii than at large ones.

Figure 4 shows the conductivity variation with pore radius at $\lambda = 18$. Each pore has 72 sulfonate groups on the wall. The numerical values in the legends are (N_L, N_c). Conductivity increases with increasing pore radius, as noted above. Pores of lower radii show a strong dependency of the proton conductivity on the sulfonate distribution. Again, a smaller radius pore provides a strong interaction force between rings of sulfonate groups and hydronium ions, thus providing a barrier to proton transport down the pore. At high values of radius, the hydronium ions are, on average, further removed from the

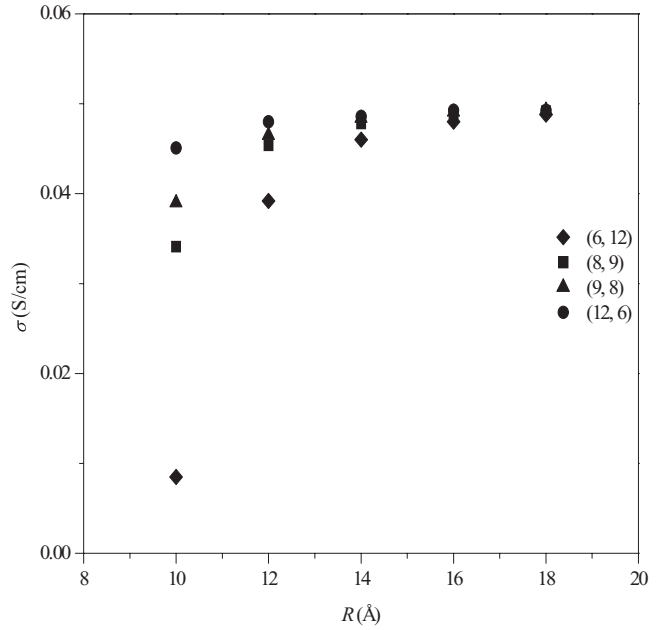

FIG. 4. Variation of conductivity (σ) with pore radius (R) at water content (λ) = 18. The numerical values in the legends are (N_L, N_c). The total number of sulfonate groups on the pore wall is 72.

sulfonate groups and, therefore, their distribution has little effect on proton conductivity.

D. Effect of N_L on conductivity

This subsection examines the conductivity of pores that have the same radius, the same number of sulfonate groups in the rings, and the same distance between two consecutive rings along the length of the pores. In this case, the volume of a pore depends on the number of rings of sulfonate groups along the length, N_L, and water content, λ, of the pore. At fixed water content, increasing the value of N_L by two will double the volume and, thus, will double the length of the pore.

The variation of conductivity with N_L is shown in Fig. 5. The conductivity data for the pores of radii 10 and 14 Å are presented. The number of sulfonate groups in each ring is 6. Each pore was considered at three water contents, 6, 12, and 18. The numerical values in the legends are (λ, R). This figure shows that the conductivities of all pores and of same water content are almost the same if the value of N_L is doubled or tripled from 6. The slight change in the conductivity data evident in this figure is due to a minor change in the value of L_z in the pore. For a pore of length L and N_L sulfonate groups, L_z is $L / (N_L - 1)$, and for a pore of length $2L$ and $2N_L$ sulfonate groups, L_z is $2L / (2N_L - 1)$; hence, the value of L_z differs slightly. Results show that the conductivity of the pore does not change significantly with N_L or with the length of the pore at a fixed radius and fixed water content. In other words, the conductivity for a specific sulfonate distribution is not much affected by the length of the pore.

E. Calculation of the flux and conductivity within two pores in series

The species enter and leave the membrane via two interfaces at the anode side and cathode side of the membrane, respectively. The pores in the interface can be different in radius and length from the pores within the membrane. The ionomer used in the MEA is of the same material as in the

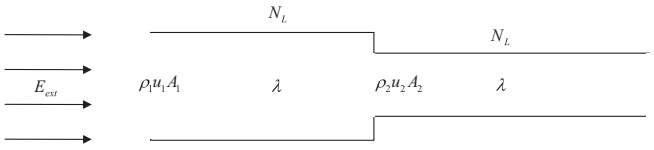

FIG. 6. Two pores of different radii in series. Each pore has N_L rings of sulfonate groups with N_c groups per ring. The water content is λ. An external field, E_{ext}, is applied.

membrane; the distribution of sulfonate ions on the pore wall will therefore be similar. The water content of the pores will also be similar. These two different kinds of pores, membrane, and interface, can be modeled as if in series, as depicted in Fig. 6. Under these conditions, the pores have equivalent volumes, provided that they are completely filled with water. The material balance in each pore dictates that the number of hydronium ions per unit time entering into each pore under the influence of external field, E_{ext}, will be the same. If the fluxes of hydronium ions in the pores are $\rho_1 u_1$ and $\rho_2 u_2$, respectively, and the cross-sectional areas are A_1 and A_2, respectively, the material balance is

$$\rho_1 u_1 A_1 = \rho_2 u_2 A_2. \tag{42}$$

The electric current, i, in the pores can be expressed in terms of hydronium ion fluxes within the pores as

$$i = \rho_1 u_1 A_1 \frac{F}{N_A} = \rho_2 u_2 A_2 \frac{F}{N_A}, \tag{43}$$

and the total conductivity of the two pores in series, σ_T, can be expressed, according to Eq. (30), as

$$\frac{1}{\sigma_T} = \frac{E_{ext}}{i/A}, \tag{44}$$

where A is the resultant cross-sectional area of the combined pores and can be related to the cross-sectional area and length of the individual pores, L_1 and L_2, as

$$A = \frac{A_1 L_1 + A_2 L_2}{L}, \tag{45}$$

where $L = L_1 + L_2$. Equation (44) can be rewritten as

$$\frac{1}{\sigma_T}\frac{L}{A} = \frac{E_{ext} L}{i}. \tag{46}$$

The total potential drop across the pores is the sum of potential drops across the individual pores; i.e., $E_{ext}L = E_{ext}L_1 + E_{ext}L_2$. Equation (46) can be further reduced by employing Eq. (43), ultimately resulting in a final expression for the overall pore conductivity:

$$\frac{1}{\sigma_T} = \frac{1}{L^2}\left(\frac{L_1^2}{\sigma_1} + \frac{L_2^2}{\sigma_2} + L_1 L_2\left(\frac{R_2^2}{\sigma_1 R_1^2} + \frac{R_1^2}{\sigma_2 R_2^2}\right)\right). \tag{47}$$

This expression shows that the resultant conductivity depends on the lengths, radii, and conductivities of the pores in series.

Assuming that both the membrane and ionomer interface have a water content of 12, the radii of the pores are 12 and 10 Å, respectively, and the number of sulfonate groups in each pore is 72. Table II presents the conductivities of these pores. Clearly, conductivity of the pore of radius 10 Å is lower, as discussed in Subsections III A–III D. The number of sulfonate groups and water content are the same in the pores; therefore, the volumes are also the same. Lengths of the pores were calculated from their volumes and radii. The resultant conductivity of the pores was determined using Eq. (47) with the knowledge of their radii, lengths, and individual conductivities, as displayed in the last column of the table. Results show that the resultant conductivity is closer to the conductivity of the small radius pore, i.e., 10 Å; thus, the pore with the lowest conductivity controls the resultant conductivity of two pores in series. This is generally the pore with the smaller radius, regardless of individual pore length. The radii of the pores in the interface are typically smaller than those in the membrane, and, thus, it is highly likely that the interface will control the total conductivity of the MEA, especially at high water contents where the membrane channels will become increasingly dilated (Fig. 6).

TABLE II. Conductivity (σ) of two individual pores (R = 10 Å and R = 12 Å) and resultant conductivity (σ_R) of the pores in series. The total number of sulfonate groups in each pore is $N_L \times N_c = 36$, where N_L and N_c are the number of rings of sulfonate groups along the length and the number of sulfonate groups in a ring, respectively. The water content (λ) of each pore is 12. The sulfonate distribution on the pore wall is the same. The volumes of the two pores are also the same; i.e., the pore of radius 10 Å is longer. L_z, L_r, and L_s are the separation distance between two consecutive rings, between two consecutive sulfonate groups in a ring, and average separation distance between two sulfonate groups on the pore wall, respectively. The resultant conductivity is closer to the conductivity of the pore of smaller radius (R = 10 Å).

		R = 10 Å				R = 12 Å				Pores in series
N_L	N_c	L_z (Å)	L_r (Å)	L_s (Å)	σ (S/cm)	L_z (Å)	L_r (Å)	L_s (Å)	σ (S/cm)	σ_R (S/cm)
6	12	16.4	5.2	8.5	0.0191	11.4	6.3	7.8	0.0384	0.0221
8	9	11.7	7.0	9.1	0.0352	8.2	8.4	8.3	0.0423	0.0361
9	8	10.3	7.9	9.1	0.0382	7.1	9.4	8.3	0.0430	0.0384
12	6	7.5	10.5	8.5	0.0420	5.2	12.6	7.8	0.0439	0.0413

IV. CONCLUSIONS

A typical pore within the interface of a hydrated Nafion membrane was modeled as a cylindrical tube with various distributions of sulfonate groups (anionic charges) along its length and circumference. The interface is very thin as compared to the membrane; thus, the variations in the water density and velocity were assumed to be negligible. The analytical expressions for the variation of density, velocity, and flux of the hydronium ions along the length of the tube were derived. The density of the hydronium ions changed sinusoidally along the length of the pore, exhibiting a maximum in the vicinity of the sulfonate groups. The expression of velocity of the hydronium ions exhibited a similar variation in the z direction, but exhibited a minimum near to the sulfonic acids end-groups, with a maximum in between axial locations of end-groups. The conductivity was related to the flux, and an expression for it was derived in terms of pore morphology and distribution of sulfonate groups.

The conductivity of the pore was investigated for pores of different radii, water contents, and sulfonate distribution schemes. The results showed that the conductivity increased

with increasing water content and increasing pore radius. The conductivity also increased with increasing the number of rings of sulfonate groups along the length of the pore, and decreased with increasing number of sulfonate groups in each ring. In a pore of fixed radius, increasing water content increases the separation distance between the sulfonate groups on the pore wall and, thus, had a negligible or adverse effect on the conductivity. The results showed that at fixed radius, fixed number of sulfonate groups in each ring, and fixed water content, the conductivity of a pore was independent of the number of rings along the length; in other words, independent of the length of the pore. The conductivity of two pores in series, one of the interface and one of the membrane, was also investigated. The resultant conductivity was closer to the conductivity of the pore with the lower conductivity; generally, the pore with the smaller radius. This could imply that the interfacial region controls the proton conductivity.

Realistically, the pores within the membrane and interfacial regions are not cylindrical tubes by any means, and the distribution of sulfonate groups within them is not symmetrical. However, it is reasonable to assume that a pore within the ionomer interface can be approximately treated as a cylinder, and that the average charge distribution, as mandated by the ionomer equivalent weight, is approximately evenly distributed along the pore wall. Hence, the model assumptions should not be overly restrictive as long as the correct number of charges is used in the calculations. This is essentially validated by the simulations, which showed that for a constant pore radius and charge distribution, the conductivity was essentially independent of the pore length. Furthermore, reasonable estimates of the pore diameter of the ionomer interface can be obtained from SAXS experiments, which is the approach that was used herein to estimate the appropriate pore sizes to use in the simulations. Consequently, for a given membrane of specified equivalent weight, a cylindrical tube with uniformly distributed charges should constitute a reasonable model for examining the effects of sulfonate distribution, water content, pore size, etc. on proton transport through a typical pore, and to approximate with reasonable accuracy macroscopic transport properties, such as the overall MEA conductivity. Hence, the model may prove very useful for estimating conductivities and other transport properties in situations that are largely inaccessible experimentally, or for examining efficiently the competing effects on PEM conductivity, such as, e.g., the dependence of conductivity on hydration level, equivalent weight, thickness of interface, and pore size.

ACKNOWLEDGMENTS

This work was supported by the Sustainable Energy Education and Research Center (SEERC) at the University of Tennessee, Knoxville.

APPENDIX A: MICROSCOPIC STATISTICAL MECHANICAL MODEL

This statistical model is based on the assumption that the water domains are regular cylindrical channels of constant diameter with uniformly distributed sulfonate groups. Microscopic interaction potential energies among water molecules, hydronium ions, and sulfonate groups were presented previously[12] and possess the forms detailed below.

1. Sulfonate–hydronium ion interaction

The sulfonate anions are assumed to form lines of charges distributed evenly in the axial direction and around the circumference of the tube wall. Each hydronium ion interacts with these lines of charges. When a unit charge q_1 is placed in a field of a row of an infinite number of charges (with unit charge q_2) aligned in the $z$direction, the potential energy of the charge q_1 changes periodically in the z direction (Fig. 1). Using a Lekner summation,[26] the potential energy, V, at a point charge can be written as

$$V(z, r_{xy}) = \frac{q_1 q_2}{\pi \varepsilon_0 L_z}\left(\sum_{n=1}^{\infty}\cos\left(2\pi n\frac{z}{L_z}\right)K_0\left(2\pi n\frac{r_{xy}}{L_z}\right)-\frac{\ln r_{xy}}{2}\right), \quad \text{(A1)}$$

where r_{xy} is the perpendicular distance of charge q_1 from the row of charges in the x and$y$ directions, L_z is the separation distance between two consecutive charges, and K_0 is the modified Bessel function of second kind and zero order. The magnitude of the potential energy is a maximum in the vicinity of the charge and a minimum in between two consecutive charges.

A hydronium ion, α, in the pore interacts with $N_L \times N_c$ sulfonate groups; i.e., N_c lines of charges, where each line has N_L sulfonate groups. Thus, the interaction potential energy, V_p, describing the interaction of the sulfonate groups with a hydronium ion, α, at a position (r, θ, z) in the pore is

$$V_p(r,\theta,z) = \frac{q_1 q_2}{\pi \varepsilon L_z}\left(\sum_{n=1}^{N_L}\cos\left(2\pi n N_L'\frac{z}{L}\right)\times\sum_{i=1}^{N_c}K_0\left(2\pi n\frac{r_{r\theta,i}}{L_z}\right)-\sum_{i=1}^{N_c}\frac{\ln\left(r_{r\theta,i}\right)}{2}\right), \quad \text{(A2)}$$

where q_1 is the charge of a hydronium ion, q_2 is the charge of a sulfonate anion, $r_{r\theta,i}$ is the perpendicular distance of the hydronium ion from the ith line charge on the pore wall, which is equal to

$$(R^2 + r^2 - 2Rr\cos(\theta_i))^{1/2}, r = [0, R], \theta_i = [0, 2\pi], \quad \text{(A3)}$$

(see Fig. 1), and ε is the permittivity of the water in the pore. The value of K_0 for $n = 1$ dominates in the summation of K_0 over $n = [1, N_c]$, so all other terms can be neglected; hence Eq. (A2) becomes

$$V_p(r,\theta,z) = \frac{q_1 q_2}{\pi \varepsilon L_z}\left(\cos\left(2\pi N_L'\frac{z}{L}\right)\sum_{i=1}^{N_c}K_0\left(2\pi\frac{r_{r\theta,i}}{L_z}\right)-\sum_{i=1}^{N_c}\frac{\ln(r_{r\theta,i})}{2}\right). \quad \text{(A4)}$$

2. Charge–charge interaction

A hydronium ion is positively charged. The interaction of a pair of hydronium ions was assumed to be Coulombic. Thus, the potential energy, $V_{\alpha\alpha}$, between two hydronium ions inside a pore is

$$V_{\alpha\alpha}(|\mathbf{r}_{\alpha_i} - \mathbf{r}_{\alpha_j}|) = \frac{q_1^2}{4\pi\varepsilon|\mathbf{r}_{\alpha_i} - \mathbf{r}_{\alpha_j}|} \tag{A5}$$

for $i \neq j$, where $|\mathbf{r}_{\alpha_i} - \mathbf{r}_{\alpha_j}|$ is the separation distance between any pair of hydronium ions, i and j.

3. Dipole–dipole interaction

We assumed that the interaction between water molecules is described by a dipole–dipole interaction and that water molecules comprise a continuum within the pore (consider the thermal distribution of water molecules); hence, the interaction energy, V_{ss}, between two water molecules having dipole moment μ is

$$V_{ss}(|\mathbf{r}_{s_i} - \mathbf{r}_{s_j}|) = -\frac{2\mu^4}{3(4\pi\varepsilon)^2 k_B T|\mathbf{r}_{s_i} - \mathbf{r}_{s_j}|^6} \tag{A6}$$

for $i \neq j$, where $|\mathbf{r}_{s_i} - \mathbf{r}_{s_j}|$ is the separation distance between any pair of water molecules.

4. Charge–dipole interaction

The interaction between a hydronium ion and a water molecule was considered to be a charge–dipole interaction. Hence, the interaction potential energy, $V_{\alpha s}$, assuming that the water molecules form a continuum and follow the thermal distribution, is

$$V_{\alpha s}(|\mathbf{r}_\alpha - \mathbf{r}_s|) = -\frac{\mu^2 q_1^2}{48\pi^2\varepsilon^2 k_B T|\mathbf{r}_\alpha - \mathbf{r}_s|^4}, \tag{A7}$$

where $|\mathbf{r}_\alpha - \mathbf{r}_s|$ is the separation distance between a hydronium ion, α, and a water molecule, s.

APPENDIX B: CONSTANTS AND DIMENSIONLESS GROUPS USED IN CALCULATIONS

The following values and units were assigned to the model parameters.

Proton diffusion coefficient in the hydrated Nafion membrane:[17,27] $D_{\rho_\alpha} = 8.0 \times 10^{-10}$ m^2/s at λ;

Viscosity of water (at 298 K): $\eta = 8.91 \times 10^{-4}$ Ns/m^2;

Temperature: $T = 298$ K;

Radius of a water molecule: $r_s = 1.5$ Å;

Radius of a hydronium ion: $r_\alpha = 1.5$ Å;

Surface charge density on the pore wall: $\Omega_s = -\frac{N_L N_c F}{2\pi R L N_A}$;

External field strength: $E_{ext,z} = 2000$ V/m[15].

The value of the velocity of hydronium ions at the pore entrance, V_α, was calculated using the Nernst-Einstein equation, which relates the diffusivity of a hydronium through a medium to its steady-state velocity by

$$V_\alpha = \frac{D_{\rho_\alpha}}{R_g T} F E_{ext,z}, \tag{B1}$$

and $\bar{\rho}_\alpha$ is the number density of hydronium ions in the pore $= \frac{N_L N_c}{\pi R^2 L N_A}$.

For a pore with specification $N_L = 10$, $N_c = 6$, and $\lambda = 10$, $L = 80$ Å, the radius of the pore can be calculated by assuming that the pore is filled with water. The calculated values of radius, surface charge density, density, velocity of hydronium ions, and the dimensionless groups are

$R = 8.5$ Å, $\Omega_s = -0.226$ C/m^2, $\bar{\rho}_\alpha = 3.35 \times 10^{27}$/m^3, $V_\alpha = 6.2 \times 10^{-3}$ cm/s, $Di_\alpha = 4.80 \times 10^{-11}$, $Hh_\alpha = 1.23 \times 10^{14}$, $Hy_\alpha = -2.82 \times 10^{12}$, $Me_\alpha = -1.23 \times 10^{16}$, $Re_\alpha = 1.24 \times 10^{-8}$, and $En_\alpha = 2.08 \times 10^{10}$.

[1] Z. X. Liang, T. S. Zhao, and J. Prabhuram, Electrochim. Acta **51**(28), 6412 (2006).
[2] S. Kim and M. M. Mench, J. Power Sources **174**(1), 206 (2007); S. Kim, B. K. Ahn, and M. M. Mench, *ibid.* **179**(1), 140 (2008).
[3] S. Kim, M. Khandelwal, C. Chacko, and M. M. Mench, J. Electrochem. Soc. **156**(1), B99 (2009).
[4] S. J. Paddison and K. S. Promislov, *Device and Materials Modelling in PEM Fuel Cells* (Springer, New York, 2009).
[5] D. M. Bernardi and M. W. Verbrugge, AIChE J. **37**(8), 1151 (1991); M. Eikerling, Y. I. Kharkats, A. A. Kornyshev, and Y. M. Volfkovich, J. Electrochem. Soc. **145**(8), 2684 (1998).
[6] T. E. Springer, T. A. Zawodzinski, and S. Gottesfeld, J. Electrochem. Soc. **138**(8), 2334 (1991).
[7] P. Kerkhof, Chem. Eng. J. **64**(3), 319 (1996).
[8] J. Fimrite, H. Struchtrup, and N. Djilali, J. Electrochem. Soc. **152**(9), A1804 (2005).
[9] T. Thampan, S. Malhotra, H. Tang, and R. Datta, J. Electrochem. Soc. **147**(9), 3242 (2000).
[10] E. A. Mason and A. P. Malinauskas, *Gas Transport in Porous Media: The Dusty Gas Model* (Elsevier, Amsterdam, 1983).
[11] X.-D. Din and E. E. Michaelides, AIChE J. **44**(1), 35 (1998); A. Vishnyakov and A. V. Neimark, J. Phys. Chem. B **104**(18), 4471 (2000); E. Spohr, P. Commer, and A. A. Kornyshev, *ibid.* **106**(41), 10560 (2002); M. K. Petersen and G. A. Voth, *ibid.* **110**(37), 18594 (2006); I. H. Hristov, S. J. Paddison, and R. Paul, *ibid.* **112**(10), 2937 (2008); S. Feng and G. A. Voth, *ibid.* **115**(19), 5903 (2011).
[12] S. J. Paddison, R. Paul, and T. A. Zawodzinski, J. Electrochem. Soc. **147**(2), 617 (2000).
[13] S. J. Paddison, R. Paul, and T. A. Zawodzinski, J. Chem. Phys. **115**, 7753 (2001); S. J. Paddison and R. Paul, Phys. Chem. Chem. Phys. **4**(7), 1158 (2002); R. Paul and S. J. Paddison, J. Chem. Phys. **123**, 224704 (2005).
[14] E. H. Cwirko and R. G. Carbonell, J. Membr. Sci. **67**(2-3), 227 (1992); S. Koter, *ibid.* **206**(1-2), 201 (2002); Y. Yang and P. N. Pintauro, Ind. Eng. Chem. Res. **43**(12), 2957 (2004); T. Colinart, S. Didierjean, O. Lottin, G. Maranzana, and C. Moyne, J. Electrochem. Soc. **155**(3), B244 (2008).
[15] P. Berg and K. Ladipo, Proc. R. Soc. London **465**(2109), 2663 (2009).
[16] A. N. Beris and B. J. Edwards, *Thermodynamics of Flowing Systems* (Oxford University Press, New York, 1994).
[17] K. D. Kreuer, J. Membr. Sci. **185**(1), 29 (2001).
[18] M. Kumar, Ph.D. dissertation (University of Tennessee, 2011).
[19] R. Qiao and N. R. Aluru, J. Chem. Phys. **118**(10), 4692 (2003).
[20] B. J. Edwards and A. N. Beris, J. Phys. A: Math. Gen. **24**(11), 2461 (1991); Ind. Eng. Chem. Res. **30**(5), 873 (1991); M. Grmela, Phys. Lett. A **102**(8), 355 (1984).
[21] R. B. Bird, W. E. Stewart, and E. N. Lightfoot, *Transport Phenomena* (Wiley, 2007).
[22] T. D. Gierke and W. Y. Hsu, *Perfluorinated Ionomer Membrane* (American Chemical Society, Washington, D.C., 1982); T. D. Gierke, G. E. Munn, and F. C. Wilson, J. Polym. Sci., Polym. Phys. Ed. **19**(11), 1687 (1981).
[23] J. S. Newman, *Electrochemical Systems* (Prentice-Hall, NJ, 1991); J. A. Wesselingh, P. Vonk, and G. Kraaijeveld, Chem. Eng. J. Bioch. Eng. **57**(2), 75 (1995).
[24] D. R. Morris and X. D. Sun, J. Appl. Polym. Sci. **50**(8), 1445 (1993).
[25] K. D. Kreuer, Solid State Ionics **97**(1-4), 1 (1997).
[26] N. Gronbech-Jensen, G. Hummer, and K. M. Beardmore, Mol. Phys. **92**(5), 941 (1997).
[27] S. J. Paddison, Annu. Rev. Mater. Res. **33**, 289 (2003).